

See discussions, stats, and author profiles for this publication at: <https://www.researchgate.net/publication/235389909>

Polymeric micelles and vesicles: Biological behavior evaluation using radiolabeling techniques

Article in *Pharmaceutical Development and Technology* · January 2013

DOI: 10.3109/10837450.2013.763264 · Source: PubMed

CITATIONS

8

READS

103

8 authors, including:



Dimitrios Psimadas

General University Hospital of Larissa

55 PUBLICATIONS 445 CITATIONS

[SEE PROFILE](#)



Hugo Oliveira

Université Victor Segalen Bordeaux 2

57 PUBLICATIONS 991 CITATIONS

[SEE PROFILE](#)



Sébastien Lecommandoux

Ecole Nationale Supérieure de Chimie, de Biologie et de Physique (ENSCBP)

220 PUBLICATIONS 8,836 CITATIONS

[SEE PROFILE](#)

Some of the authors of this publication are also working on these related projects:



NanoTHER [View project](#)



Nuclear Cardiology [View project](#)

SHORT REPORT

Polymeric micelles and vesicles: biological behavior evaluation using radiolabeling techniques

Dimitrios Psimadas^{1,2,3}, Hugo Oliveira^{4,5}, Julie Thevenot^{4,5}, Sebastien Lecommandoux^{4,5}, Penelope Bouziotis², Alexandra D. Varvarigou², Panagiotis Georgoulas³, and George Loudos¹

¹Department of Medical Instruments Technology, Technological Educational Institute of Athens, Egaleo, Athens, Greece, ²Institute of Nuclear and Radiological Sciences and Technology, Energy & Safety, NCSR "Demokritos", Aghia Paraskevi, Athens, Greece, ³Department of Nuclear Medicine, University Hospital of Larissa, Mezourlo, Larissa, Greece, ⁴IPB, ENSCBP, University of Bordeaux, Pessac Cedex, France, and ⁵Laboratory of Organic Chemistry Polymers (UMR5629), CNRS, Pessac Cedex, France

Abstract

The application of combined diagnosis and therapy through nanotechnology applications is attracting increasing attention worldwide. Polymeric self-assembled nanoparticles (NPs) have been studied for this purpose. Micelles and vesicles with or without a magnetic core can efficiently carry diagnostic and/or therapeutic agents to a desired target. The biological behavior of these NPs has been evaluated in this study, after radiolabeling with ^{99m}Tc. *In vitro* stability, in media that mimic the environment of the living body, was better for vesicles than for micelles at 1 h and decreased for both as time passed. After administration to healthy animals, all NPs presented major uptake at liver and spleen as expected. Biodistribution and imaging studies confirmed the higher uptake in these organs for the hybrid NPs and at higher extent for the ones with larger size, indicating that the magnetic load and size play an important role on *in vivo* distribution.

Keywords

Biodistribution, imaging, nanoparticles, technetium

History

Received 12 November 2012
Revised 24 December 2012
Accepted 27 December 2012
Published online ■■■

Introduction

The dynamic combination of therapeutic and diagnostic research utilities (theranostics) can offer significant benefits in medicine, such as guided molecular therapy and personalized medical care. To render cancer theranostics possible, it is essential to develop multifunctional tumor-targeting nanocarriers with combined diagnostic and therapeutic effect¹. Particles of various materials and structures, with dimensions at the nanometer scale (nanoparticles, NPs), designed to incorporate a wide variety of chemotherapeutic and diagnostic agents for their delivery to tumor cells, exhibit several advantages over conventional delivery systems². Having high stability, high drug loading and controlled release capacity, the potential to incorporate both hydrophilic and hydrophobic substances and being possibly administered through variable routes, NPs can produce considerable pharmacological action with reduction of the dosing frequency.

It is well known that certain amphiphilic block copolymers can form nanoassemblies of micelles and vesicles in an aqueous solution, depending on their chemical structures and relative hydrophilicity/hydrophobicity³. Considerable interest has been attracted by polymeric micelles due to their unique characteristics such as core-shell structure, mesoscopic size range and prolonged blood circulation⁴. Lipophilic anticancer drugs can be encapsulated to the hydrophobic inner core, while the outer hydrophilic flexible shell plays a key role in the stabilization of the

drug-carried micelle. Polymer vesicles are also promising systems for either hydrophilic or hydrophobic drug delivery applications and may offer many advantages compared to low molar-mass lipid vesicles, such as enhanced stability and control of their physical, chemical and biological properties by tailoring the block lengths⁵. Development of vesicles that respond to internal or external stimuli such as temperature, pH, oxidative stress, light, magnetic fields and ultrasound has been highly promoted⁶. In addition, both micelles and vesicles can be surface functionalized with various targeting ligands offering new prospects to the NPs formed⁶. Much attention has recently been paid to the study of hybrid micelle and vesicle NPs containing magnetic cores for biomedical application, due to their particularly large surface-to-volume ratio, quantum size effect, strong interaction with high-frequency electromagnetic fields and low toxicity⁷.

In general, upon administration in the body, the NP behavior can only be partially predicted according to existing research experience and based on their size and surface properties. In biological environments, due to the adsorption of biomolecules (e.g. proteins and lipids) at the NP surface, opsonization takes place and should be taken into account due to its major role in the final *in vivo* behavior⁸. Since interactions between NPs and their surroundings are important factors that can determine their potential biomedical applications, it is important to examine their *in vivo* performance and to establish eventual differences between hybrid micelle and vesicle nanoassemblies.

Here, in order to visualize the NPs' fate *in vivo* and to obtain an accurate biodistribution profile, NPs were labeled with a detectable radioactive probe. Radioactive NPs were then used for two purposes: measurement of radioactivity in various tissues following administration allowing a quantitative biodistribution

Address for correspondence: Dimitrios Psimadas, Department of Nuclear Medicine, University Hospital of Larissa, Mezourlo 41110, Larissa, Greece. Tel: +30 241 3502916. Fax: +30 241 3501863. E-mail: dpsimad@chem.uoa.gr

study, and dynamic γ or PET imaging of the whole body (or acquisitions at predetermined time periods)^{8,9}. The most commonly used γ -emitting radionuclide in Nuclear Medicine is ^{99m}Tc due to its convenient 6-h half-life, its appropriate 140 keV γ -energy and its widespread availability. NPs can be efficiently radiolabeled with ^{99m}Tc with chemical modifications that have a negligible effect in their original structure¹⁰.

Our objective was to perform a comparative study regarding the biological properties of micelles and vesicles obtained by self-assembly of biodegradable, stimuli-responsive, amphiphilic, poly(amino acid)-based block copolymers. For this purpose, biodistribution and scintigraphic analyses were performed after ^{99m}Tc -radiolabeling of poly(ethylene glycol)-*block*-poly(γ -benzyl-L-glutamate) (PEG-*b*-PBLG) micelles (NP3) and poly(trimethylene carbonate)-*block*-poly(glutamic acid) (PTMC-*b*-PGA) vesicles (NP13). Identical studies were performed using the same NPs containing a 12 nm $\gamma\text{-Fe}_2\text{O}_3$ magnetic core (HNP3 and HNP13, respectively).

Methods

Materials

PTMC-*b*-PGA polymersomes and hybrid polymersomes were obtained by the nanoprecipitation method (solvent-assisted dispersion) according to previously published procedures^{11,12}. PEG-*b*-PBLG was synthesized according to a protocol described elsewhere with minor modifications¹³. PEG-*b*-PBLG and hybrid micelles were obtained by nanoprecipitation in ultrapure water using a similar protocol as the one implemented for PTMC-*b*-PGA polymersomes. All particles were purified by extensive dialysis against ultrapure water. Final concentrations of the dispersions were adjusted by ultrafiltration using a Millipore stirred cell (4 bar nitrogen pressure, regenerated cellulose membrane MWCO 100 000 Da). Particle size was measured by dynamic light scattering with the NanoZS90 device from Malvern Instruments. The sample was kept at constant temperature (25 °C) during the experiment. Measurement was carried out at 90 °C. The data acquisition was done using the automatic adjustment of position, attenuation and measurement time. Three measurements gave the average value of the mean hydrodynamic diameter (obtained from the cumulate analysis).

The ^{99}Mo - ^{99m}Tc generator was from Mallinckrodt Medical BV and the dose calibrator from Capintec. ITLC sheets were purchased from Gelman Sciences and radio ITLC analysis was performed on a Packard Imager (Canberra). Biodistribution samples radioactivity was measured in a CobraII γ -counter from Packard, Canberra. The chemicals and reagents used were of analytical grade.

Radiosynthesis and stability of the ^{99m}Tc -NP complexes

All four NPs were directly radiolabeled with ^{99m}Tc using SnCl_2 as reducing agent according to a method already described⁹. Briefly, fresh $\text{Na}^{99m}\text{TcO}_4$ generator eluate (~1–2 mCi) was reduced with SnCl_2 (40 μg) and the pH was adjusted to neutral. Aliquots of NP

solution containing 200 μg of NPs were added and the reaction mixture was left at RT for 45 min. Quality control of the ^{99m}Tc -NP complexes was performed with ITLC-SG, using acetone and a mixture of pyridine:acetic acid:water (3:5:1.5) as the mobile phases¹⁰.

In order to evaluate the strength of the bonding of ^{99m}Tc with the NPs and consequently the stability of the complex, 50 μl of each of the labeled preparation was challenged against 450 μl of histidine (His) and DTPA solutions (0.01 M) as well as against serum. The sample mixture was incubated at 37 °C for 1, 3 and 24 h and analyzed by ITLC-SG.

Radiobiological and scintigraphic studies

Radiolabeled NPs (100 μl –1 mCi/ml) were evaluated *in vivo* after i.v. administration in normal female Swiss mice via the tail vein. Biodistribution studies were performed at 3 min, 1 h and 24 h p.i. The principal organs as well as muscle samples were removed, washed, dried, weighed and counted in a γ -counter, together with collected urine samples. The percentage of the injected dose per organ (% ID/organ) and the injected dose per gram of tissue (% ID/g) were calculated, in reference to a standard of the injected solution. For imaging studies, the animals were anaesthetized right after injection, using a mixture of 0.5 ml of ketamine hydrochloride (100 mg/ml), 0.25 ml of xylazine (20 mg/ml) and 4.25 ml of NaCl 0.9% (dose: 0.1 ml/10 g of animal weight administered intraperitoneally). Dynamic images of the injected mice were obtained from 10–60 min p.i. using a high-resolution γ -camera system described elsewhere⁹. *In vivo* studies were performed in compliance with European legislation and Greek authorities have approved all animal protocols.

Results and discussion

Radiochemical analysis

The NPs studied are presented in Table 1. The radiolabeling of all four NPs was efficiently performed at high yields (>98%) by applying the direct methodology, as neither free pertechnetate nor radiocolloids were observed in the final preparation.

Challenge stability studies were evaluated by ITLC-SG using different mobile solvent phases in order to separate the different radiolabeled species and calculate the remaining intact ^{99m}Tc -NP complex. Using acetone as the mobile phase free pertechnetate which have Rf: 1 can be separated from all labeled species (^{99m}Tc -NPs, ^{99m}Tc -His and ^{99m}Tc -DTPA) and large radiocolloids ($^{99m}\text{TcO}_2$) which have Rf: 0. Two additional mobile phase solvents were applied for the ITLC-SG analysis; saline 0.9% for the His and DTPA challenge, and a mixture of pyridine:acetic acid:water (3:5:1.5) for serum stability. In normal saline ^{99m}Tc -His and ^{99m}Tc -DTPA complexes as well as free $^{99m}\text{TcO}_4^-$ migrate to Rf: 0.8–1 while the ^{99m}Tc -NPs complex remains at Rf: 0 and in the pyridine mixture large radiocolloids remain at Rf: 0 while all other radioactive species migrate to Rf: 0.8–1^{9,14}.

Table 1. The characteristics of the NPs studied.

NP	Self-assembly morphology	Polymer composition	Mean hydrodynamic diameter (nm)	Iron oxide content	Radiolabeling yield (%)
NP3	Micelles	PEG- <i>b</i> -PBLG	70	No	>98
NP13	Vesicles	PTMC- <i>b</i> -PGA	107	No	>98
HNP3	Micelles	PEG- <i>b</i> -PBLG	121	20% w/w of 12 nm $\gamma\text{-Fe}_2\text{O}_3$ maghemite	>98
HNP13	Vesicles	PTMC- <i>b</i> -PGA	140	20% w/w of 12 nm $\gamma\text{-Fe}_2\text{O}_3$ maghemite	>98

Results are shown in Figure 1. While His challenge revealed high stability for all radiolabeled NPs, DTPA challenge showed that the NP13 and HNP13 vesicles were more stable than the NP3 and HNP3 micelles. After 1 h incubation with DTPA, NP13 ($37 \pm 6\%$) and its hybrid analog HNP13 ($31 \pm 8\%$) were the most stable of all the four NP formulations, while the two micelles (NP3: $20 \pm 5\%$ and HNP3: $16 \pm 6\%$) had the lowest stability. At 24 h, all NPs revealed almost complete transchelation in DTPA and minimal presence of intact ^{99m}Tc -NPs. DTPA is a very strong chelator for ^{99m}Tc , so displacement of some degree is expected. The difference in stability between the two self-assembly morphologies can be attributed to their difference in surface charge (vesicles are anionic while micelles are almost neutral) which may result a better ‘‘environment’’ for the formation of the ^{99m}Tc -complex. Serum stability studies showed that no release of ^{99m}Tc occurs from the complexes even after incubation for 24 h as demonstrated by the quality control using acetone. Nevertheless,

they form new and larger radio-complexes after attachment to serum components (e.g. large proteins), even after 1 h incubation, as it is indicated by the pyridine mixture quality control (Figure 1). It is expected that in a biological environment there are many biomolecules that compete for the limited NP-surface, altering their initial characteristics (e.g. overall size, morphology, etc.). No major differences between the radiolabeled micelles and vesicles were observed in the percentage of the remaining intact ^{99m}Tc -NPs after serum stability studies.

Biodistribution and imaging studies

Normal mice biodistribution results at 1 h p.i. are graphically presented in Figure 2. As it is expected, all four ^{99m}Tc -labeled NPs were mainly concentrated in the mononuclear phagocyte system (liver and spleen). This happens because the surface coating polymers are rich in chemical groups (e.g. $-\text{OH}$,

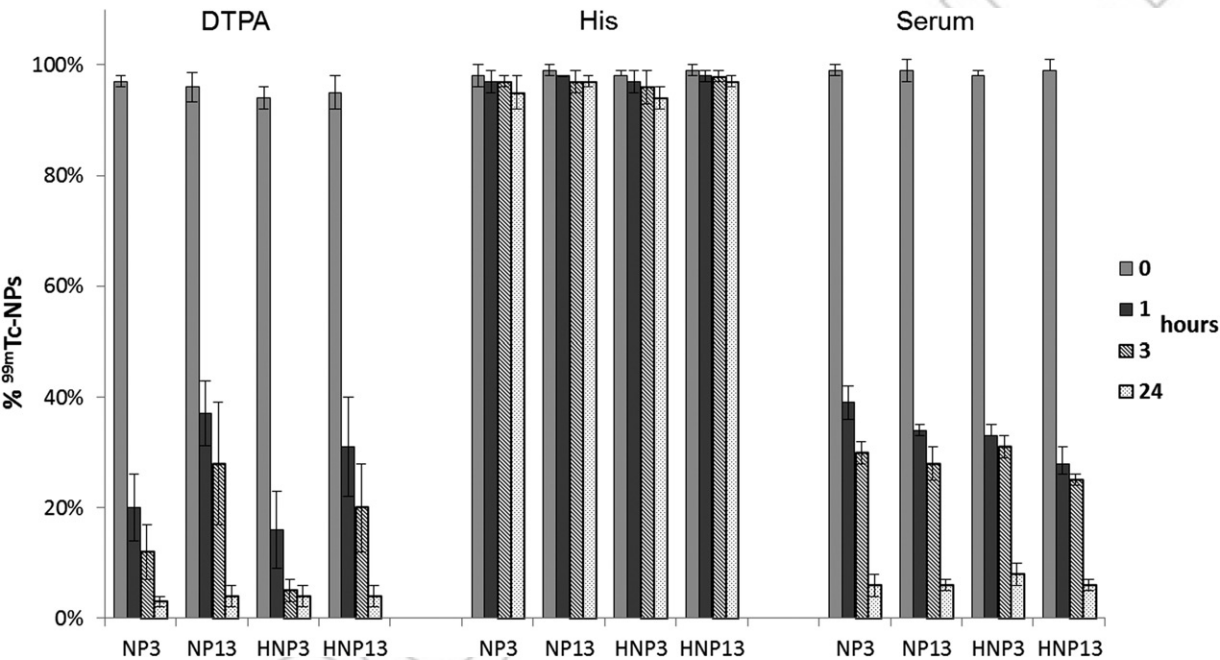


Figure 1. ITLC-SG results presenting the intact ^{99m}Tc -NPs after DTPA, His and serum stability studies, when incubated for 1, 3 and 24 h at 37°C .

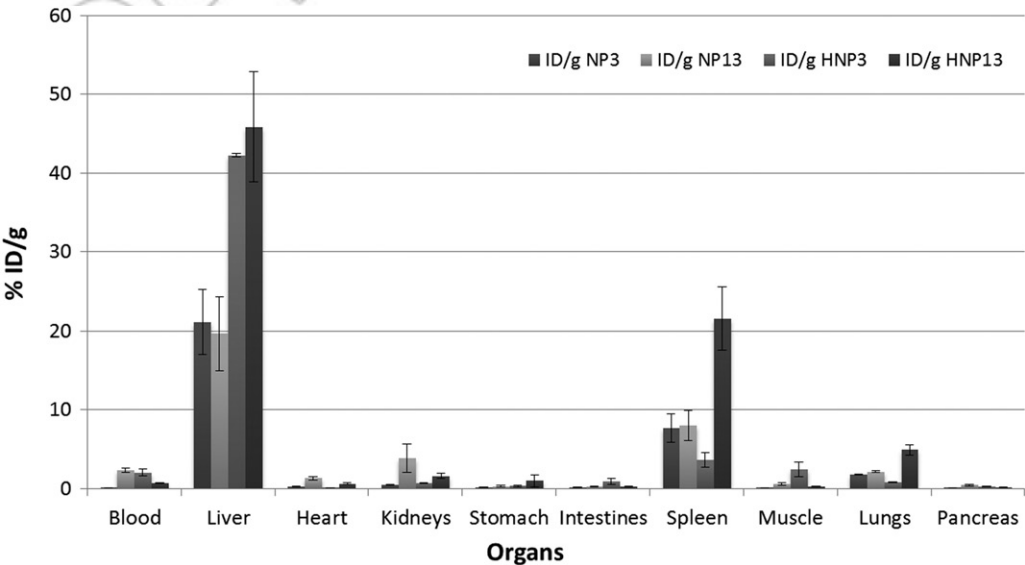


Figure 2. Biodistribution results of the radiolabeled NPs in normal mice at 1 h p.i.

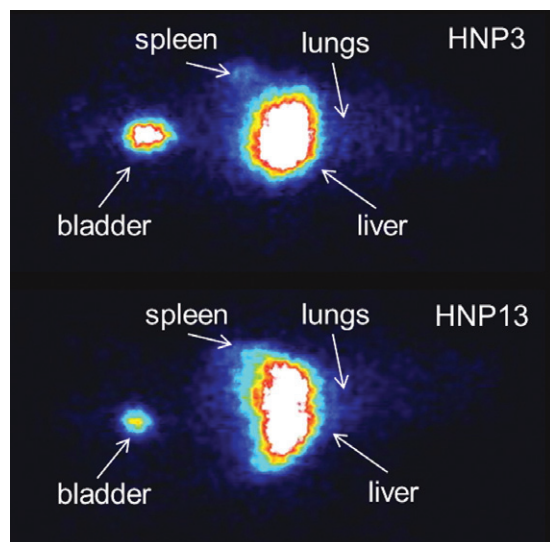


Figure 3. Scintigraphic images of the hybrid radiolabeled NPs in normal mice at 1 h p.i.

–COOH) that trigger the activation of both pathways of the complement system, initially resulting in fast opsonization after i.v. administration and eventually in macrophage uptake^{9,15}. No differences between micelle and vesicle uptake were observed in the liver, but substantial differences between hybrid and non-hybrid NPs can be detected. This may be attributed to their considerable size difference as well as to their maghemite content which limits or hinders water access to the core, resulting in significantly longer degradation rates, as reflected by their increased liver half-life⁷.

Fast blood clearance (<6% ID/g for all ^{99m}Tc-NPs at 3 min p.i.) and minimal uptake in other major organs was observed. Heart and kidney uptake at 1 h p.i. was not substantial, indicating the potential use of these NPs for anticancer drug delivery with minimum cardiac and kidney toxicity¹⁴. The lower kidney uptake, in relation to liver, observed for all NPs can be attributed to possible reabsorption before clearance⁸. Interestingly, the uptake in lungs and spleen for the largest NPs, namely the hybrid vesicle HNP13, was the highest among all four NPs at the tested time-points, suggesting most probably the formation of aggregates *in vivo*¹⁶.

In vivo stability of all radiolabeled complexes was found to be satisfactory, as the percentage of free pertechnetate which accumulates in the stomach was found to be below 1% at all time-points after a 24-h period. These results exclude the *in vivo* decomposition of the radiolabeled NP complexes into free pertechnetate which was also shown by the above *in vitro* stability studies, when mild conditions were applied.

Scintigraphic images after injection of the radiolabeled NPs in normal mice revealed high abdominal radioactivity, which is attributed to the liver and spleen uptake. This is in accordance with the biodistribution data as well as with previous findings¹⁷. The images obtained 1 h after administration of the radiolabeled hybrid NPs in healthy animals are shown in Figure 3. The increased uptake of HNP13, when compared to HNP3, in liver, spleen and lungs, which was revealed by the biodistribution analysis is also observed scintigraphically. The urinary bladder is also visible due to urinary excretion of the NPs.

Conclusion

The behavior of hybrid and non-hybrid vesicular and micellar nanoassemblies was evaluated after radiolabeling, in

conditions which mimic the biological environment as well as after injection to experimental animals. Vesicles were superior in terms of *in vitro* stability, whereas during *in vivo* biodistribution and imaging evaluation some differences were observed between the hybrid and non-hybrid NPs. Additionally, higher uptake was observed in liver, spleen and lungs for hybrid vesicles when compared to hybrid micelles. The above data confirm that vesicle structures are more stable than micelles and that size and magnetic load are parameters that play critical role in NP organ distribution profile. Therefore, the design and synthesis of small vesicle structures, with or without a magnetic loading, could be able to provide NPs with theranostic potentiality.

Acknowledgements

The authors thank Stavros Xanthopoulos for his expert assistance with the animal studies and Dr Theodoros Tsotakos for constructive discussion.

Declaration of interest

The authors report no conflicts of interest. The authors alone are responsible for the content and writing of this article.

Financial support was provided by the European Commission through the Seventh Framework Program (FP7) for Research & Development (CP-IP 213631-2 NANOTHER).

References

- Yang X, Grailer JJ, Pilla S, et al. Multifunctional polymeric vesicles for targeted drug delivery and imaging. *Biofabrication* 2010;2:025004.
- Riehemann K, Schneider SW, Luger TA, et al. Nanomedicine challenge and perspectives. *Angew Chem Int Ed Engl* 2009;48:872–97.
- Discher DE, Ahmed F. Polymersomes. *Annu Rev Biomed Eng* 2006;8:323–341.
- Jabr-Milane L, van Vlerken L, Devalapally H, et al. Multi-functional nanocarriers for targeted delivery of drugs and genes. *J Control Release* 2008;130:121–8.
- Egli S, Schlaad H, Bruns N, Meier W. Functionalization of block copolymer vesicle surfaces. *Polymers* 2011;3:252–80.
- Rezaei SJ, Nabid MR, Niknejad H, Entezami AA. Folate-decorated thermoresponsive micelles based on star-shaped amphiphilic block copolymers for efficient intracellular release of anticancer drugs. *Int J Pharm* 2012;437:70–9.
- Schlachter EK, Widmer HR, Bregy A, et al. Metabolic pathway and distribution of superparamagnetic iron oxide nanoparticles: *in vivo* study. *Int J Nanomedicine* 2011;6:1793–800.
- Sa LT, Albernaz Mde S, Patricio BF, et al. Biodistribution of nanoparticles: initial considerations. *J Pharm Biomed Anal* 2012;70:602–4.
- Psimadas D, Baldi G, Ravagli C, et al. Preliminary evaluation of a ^{99m}Tc labeled hybrid nanoparticle bearing a cobalt ferrite core: *in vivo* biodistribution. *J Biomed Nanotechnol* 2012;8:575–85.
- Psimadas D, Bouziotis P, Georgoulis P, et al. Radiolabeling approaches of nanoparticles with ^{99m}Tc. *Contrast Media Mol Imaging* (in press).
- Sanson C, LeMeins J-F, Schatz C, et al. Biocompatible and biodegradable poly(trimethylene carbonate)-b-poly(L-glutamic acid) polymersomes: size control and stability. *Langmuir* 2010;26:2751–60.
- Sanson C, Diou O, Thevenot J, et al. Doxorubicin loaded magnetic polymersomes: theranostic nanocarriers for MR imaging and magneto-chemotherapy. *ACS Nano* 2011;5:1122–40.
- Barbosa MEM, Montembault V, Cammas-Marion S, et al. Synthesis and characterization of novel poly(γ-benzyl-L-glutamate) derivatives tailored for the preparation of nanoparticles of pharmaceutical interest. *Polym Int* 2007;56:317–24.

14. Snehalatha M, Venugopal K, Saha RN, et al. Etoposide loaded PLGA and PCL nanoparticles II: biodistribution and pharmacokinetics after radiolabeling with Tc-99m. *Drug Deliv* 2008;15:277–87.
15. Stolnik S, Heald SR, Neal J, et al. Polylactide-poly(ethylene glycol) micellar-like particles as potential drug carriers: production, colloidal properties and biological performance. *J Drug Target* 2001;9:361–78.
16. Reddy LH, Sharma RK, Chuttani K, et al. Etoposide-incorporated tripalmitin nanoparticles with different surface charge: formulation, characterization, radiolabeling, and biodistribution studies. *AAPS J* 2004;6:55–64.
17. Helbok A, Rangger C, von Guggenberg E, et al. Targeting properties of peptide-modified radiolabeled liposomal nanoparticles. *Nanomedicine* 2012;8:112–18.